

# Temporal incoherent solitons supported by a defocusing nonlinearity with anomalous dispersion

Claire Michel<sup>1</sup>, Bertrand Kibler<sup>2</sup>, Josselin Garnier<sup>3</sup>, and Antonio Picozzi<sup>2</sup>

<sup>1</sup>*Laboratoire de Physique de la Matière Condensée, CNRS - Université de Nice Sophia-Antipolis, 06108 Nice, France*

<sup>2</sup>*Laboratoire Interdisciplinaire Carnot de Bourgogne, CNRS-Université de Bourgogne, Dijon, France*

<sup>3</sup>*Laboratoire de Probabilités et Modèles Aléatoires, Université Paris VII, 75205 Paris, France*

We study temporal incoherent solitons in noninstantaneous response nonlinear media. Contrarily to the usual temporal soliton, which is known to require a focusing nonlinearity with anomalous dispersion, we show that a highly noninstantaneous nonlinear response leads to incoherent soliton structures which require the inverted situation: In the focusing regime (and anomalous dispersion) the incoherent wave-packet experiences an unlimited spreading, whereas in the defocusing regime (still with anomalous dispersion) the incoherent wave-packet exhibits a self-trapping. These counterintuitive results are explained in detail by a long-range Vlasov formulation of the problem.

PACS numbers: 42.65.Tg, 42.65.Sf, 05.45.Yv

*Introduction* – Solitons have been usually considered as coherent localized structures and the discovery of incoherent optical solitons has represented a significant advance in nonlinear physics [1–4]. The incoherent soliton (IS) consists of a phenomenon of *spatial self-trapping* of incoherent light in a focusing nonlinear medium characterized by a slow response [1–4]. The remarkable simplicity of experiments realized in photorefractive crystals has led to a fruitful investigation of the dynamics of incoherent nonlinear waves [2–5]. The mechanism underlying the formation of these IS states finds its origin in the existence of a self-consistent potential, which is responsible for a spatial self-trapping of the incoherent optical beam. From this point of view, these ISs are of the same nature as the ISs predicted in plasma physics long time ago in the framework of the Vlasov equation [6–11].

Since their first experimental observation [1], ISs have been studied in different circumstances [12, 13], and have been shown to be also supported by a spatial nonlocal nonlinearity, instead of the traditional noninstantaneous nonlinearity [14, 15]. A nonlocal nonlinearity is encountered in various nonlinear wave systems [16, 17]. In particular, in the highly nonlocal limit where the range of the nonlocal response is much larger than the size of the optical beam, the beam can be guided by the nonlocal response of the material, a process originally termed ‘accessible solitons’ in Refs.[17, 18]. In this limit, a speckled beam can be guided and trapped by the effective waveguide induced by the nonlocal response [14].

From a different perspective, the long-term evolution of a modulationally unstable coherent wave has been recently studied in the presence of a nonlocal response [15]. Contrarily to the expected soliton turbulence process where a coherent soliton is eventually generated in the midst of small-scale fluctuations [19], a highly nonlocal response leads to a process of IS-turbulence, which is characterized by the spontaneous formation of an IS structure starting from an initially homogeneous plane-wave. A kinetic approach of the problem revealed that these ISs can be described by a long-range Vlasov-like equation [15].

In this article we study the existence of ISs in the temporal domain in the presence of a highly noninstantaneous nonlinear response. We report a remarkable and unexpected result: Contrarily to the spatial domain, in which IS are exclusively supported by a focusing nonlinearity, we show

that IS are exclusively supported by a defocusing nonlinearity in the temporal domain. In other terms, contrarily to the expected temporal soliton behavior, which is known to require a focusing nonlinearity with anomalous dispersion (or a defocusing nonlinearity with normal dispersion), we report here the existence of an IS which requires the inverted situation: In the focusing regime (with anomalous dispersion) the incoherent wave-packet experiences an unlimited temporal spreading, whereas in the defocusing regime (still with anomalous dispersion) the incoherent wave-packet exhibits a phenomenon of IS self-trapping.

The mechanism underlying this counterintuitive process of self-trapping finds its origin in the spectral shift induced by the causality condition inherent to the nonlinear response function – a well-known effect in the context of the Raman induced soliton self-frequency-shift [4]. When combined with natural wave dispersion, such a spectral shift leads to a constant acceleration of the IS, which in turn is responsible for a fictitious force that leads to a trapping of the incoherent wave-packet. This mechanism of acceleration-induced incoherent self-trapping in the defocusing regime, as well as the inhibition of self-trapping in the focusing regime, are explained in detail by the long-range Vlasov formalism. Note that this long-range Vlasov approach differs from the traditional Vlasov equation considered to study incoherent modulational instability and ISs in plasmas [6, 20], hydrodynamics [21] and optics [7–11]. We can expect the experimental observation of this unexpected phenomenon of self-trapping thanks to the recent progress made on the fabrication of photonic crystal fibers filled with molecular liquids displaying highly noninstantaneous Kerr responses [22].

*Numerical simulations*– We consider the standard NLS equation accounting for a noninstantaneous nonlinear response function

$$i\partial_z\psi + \partial_{tt}\psi + \sigma\psi \int R(t-t') |\psi|^2(z, t') dt' = 0. \quad (1)$$

For convenience, we normalized the equation with respect to the ‘healing time’  $\tau_0 = \sqrt{|\beta|/(|\gamma|\rho)}$  and the length scale  $L_0 = 1/(|\gamma|\rho)$ , where  $\beta$  is the dispersion coefficient,  $\beta > 0$  ( $\beta < 0$ ) referring to the anomalous (normal) dispersion regime, and  $\gamma$  is the nonlinear coefficient with  $\sigma = \text{sign}(\gamma)$ . The parameter  $\rho = \mathcal{N}/T$  is the wave intensity, which is a

conserved quantity of Eq.(1),  $\mathcal{N} = \int |\psi|^2 dt$  being the power and  $T$  the numerical temporal window. The variables can be recovered in real units through the transformations  $t \rightarrow t\tau_0$ ,  $z \rightarrow zL_0$ ,  $\psi \rightarrow \psi\sqrt{\rho}$  and  $R(t) \rightarrow \tau_0 R(t)$ . The response function  $R(t)$  is constrained by the causality condition. In the following we use the convention that  $t > 0$  corresponds to the leading edge of the pulse, so that the causal response will be on the trailing edge of a pulse, i.e.,  $R(t) = 0$  for  $t > 0$ . The range of the noninstantaneous response  $R(t)$ , say  $\tau_R$ , denotes the response time of the nonlinearity. We consider here the highly noninstantaneous nonlinear regime,  $\tau_R \gg 1$ , where the response time is much larger than the healing time or the time correlation of the optical wave [23]. In order to make easier the comparison with spatial nonlocal effects, we implicitly assumed in Eq.(1) that the wave propagates in the anomalous dispersion regime ( $\beta > 0$ ), and we will consider separately the focusing ( $\sigma = +1$ ) and defocusing ( $\sigma = -1$ ) regimes of interaction.

We report in the left columns of Fig. 1 and 2 the evolutions of the spectrograms [24] of an initial super-Gaussian incoherent wave-packet which has been obtained by integrating numerically the NLS Eq.(1). The corresponding spectral and temporal FWHM are  $\Delta_\omega = 1.257$  and  $\Delta_t = 200$ , respectively. We considered in this example a Gaussian-like response function,  $R(t) = H(-t)t^2 \exp[-t^2/(2\tau_R^2)]/(\tau_R^3 \sqrt{\pi/2})$  [ $H(t)$  being the Heaviside function], while similar results are obtained with an exponential-shaped response function. Note that the prefactor  $t^2$  avoids discontinuities in the derivative of  $R(t)$  at  $t = 0$ , which is important in order to accurately simulate the Vlasov Eq.(2). We remark in Fig. 1 that in the focusing regime ( $\sigma = +1$ ), the incoherent wave-packet exhibits a delocalization process characterized by an unlimited temporal spreading of the pulse and a slow process of spectral broadening. In marked contrast with this dispersive behavior, in the defocusing regime ( $\sigma = -1$ , see Fig. 2) the incoherent wave-packet exhibits a phenomenon of self-trapping, which is very robust and thus preserved for long propagation distances – in the example of Fig. 2 the IS loses less than 0.1% of its power while it propagates over more than  $z = 10^3$ . Note that the spectral shift of the optical wave simply results from the causality property of  $R(t)$ . This effect is well-known for the Raman induced self-frequency-shift [4, 13], and manifests itself as a red- (blue-)shift in the focusing (defocusing) nonlinear regime [25].

*Vlasov approach* – This novel phenomenon of incoherent self-trapping is explained in detail by the ‘long-range’ Vlasov equation [26, 27], which describes the evolution of the averaged local spectrum of the wave,  $n_\omega(t, z) = \int B(t, \tau, z) \exp(i\omega\tau) d\tau$ , where  $B(t, \tau, z) = \langle \psi(t - \tau/2, z) \psi^*(t + \tau/2, z) \rangle$  is the correlation function and  $\langle \cdot \rangle$  denotes an average over the realizations

$$\partial_z n_\omega(t, z) + \partial_\omega \tilde{k}_\omega(t, z) \partial_t n_\omega(t, z) - \partial_t \tilde{k}_\omega(t, z) \partial_\omega n_\omega(t, z) = 0, \quad (2)$$

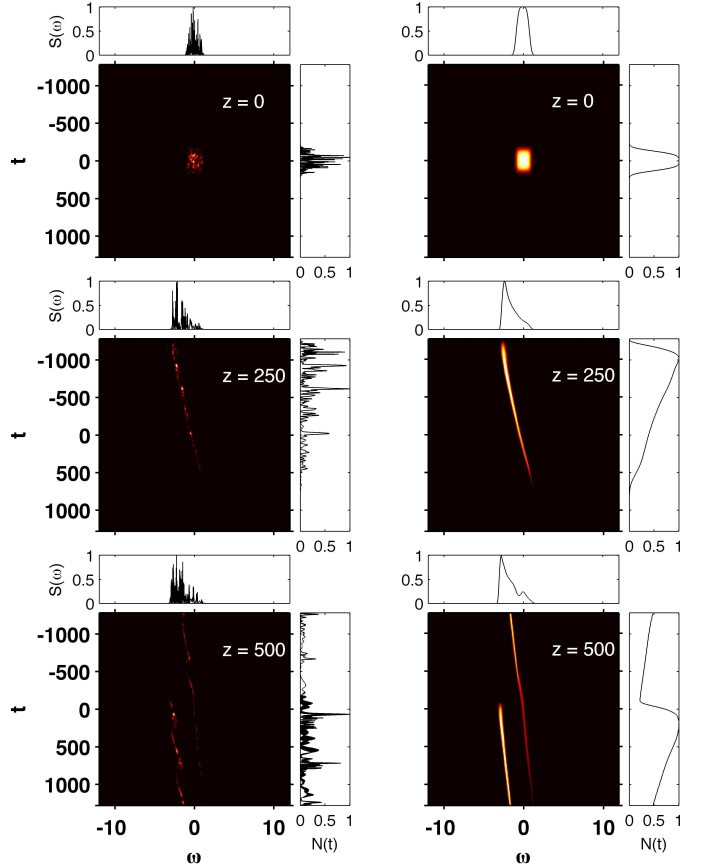


FIG. 1: Evolutions of the spectrogram (left column), and of the local spectrum  $n_\omega(t, z)$  (right column), obtained by integrating numerically the NLS Eq.(1) and the Vlasov Eq.(2), respectively. The simulations refer to a focusing nonlinearity in the anomalous dispersion regime,  $\sigma = +1$  [ $\tau_R = 200$  (in units of  $\tau_0$ )].

where  $\tilde{k}_\omega(t, z) = k(\omega) + V(t, z)$  is the generalized dispersion relation, with  $k(\omega) = \omega^2$ , and the self-consistent potential  $V(t, z) = -\sigma R * N$ , where  $*$  denotes the temporal convolution product and  $N(t, z) = (2\pi)^{-1} \int n_\omega(t, z) d\omega$  the averaged intensity profile of the incoherent wave. The structure of Eq.(2) is analogous to the Vlasov equation recently derived to describe highly nonlocal spatial effects [15]. Note however that in the temporal domain the potential  $V(t, z)$  is constrained by the causality property of  $R(t)$ , which breaks the Hamiltonian structure of the Vlasov Eq.(2).

We report in the right columns of Fig. 1 and 2 the simulations of the Vlasov Eq.(2) starting from the same initial condition as the NLS Eq.(1). We underline the good agreement between the NLS and Vlasov simulations, which corroborates the fact that the ‘long-range’ Vlasov Eq.(2) provides an ‘exact’ statistical description of the random nonlinear wave (see Ref.[15]). Figure 3 remarkably reveals that, after a transient ( $z \sim 300$ ), the wave-packet adopts an invariant profile characterized by a linear spectral shift, which in turn induces a constant IS acceleration (parabolic trajectory) in the temporal domain. Note that in a real experiment, this spectral shift can be affected by the particular form of the dispersion of the PCF [22], so that an improved NLS model accounting for higher-order dispersion effects should be considered.

To discuss the mechanism underlying the formation of

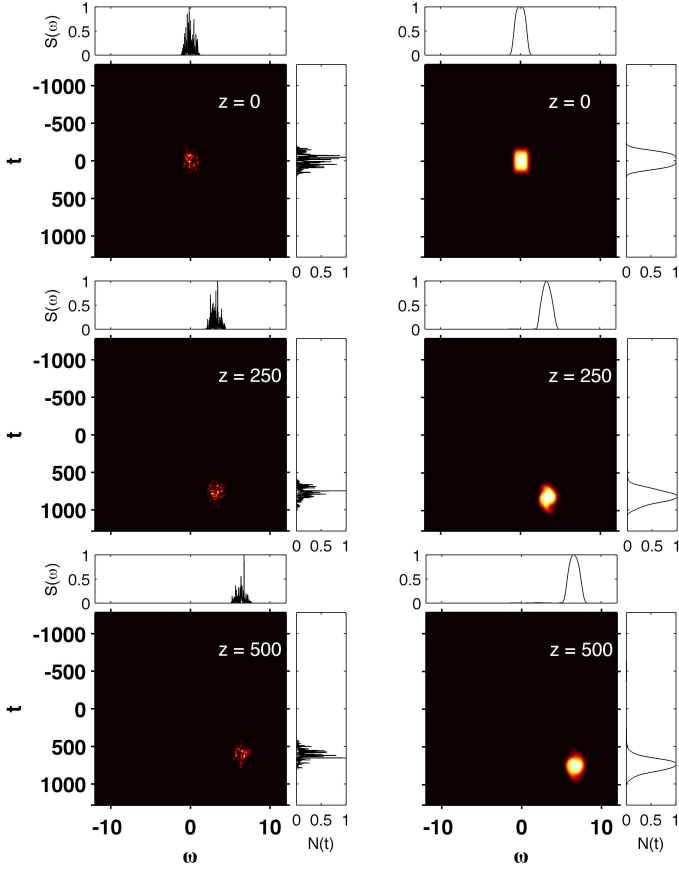


FIG. 2: Evolutions of the spectrogram (left column), and of the local spectrum  $n_\omega(t, z)$  (right column), obtained by integrating numerically the NLS Eq.(1) and the Vlasov Eq.(2), respectively. The simulations have been performed with a defocusing nonlinearity in the anomalous dispersion regime – parameters and initial conditions are the same as in Fig. 1, except that  $\sigma = -1$ . After a transient ( $z \sim 300$ ), the incoherent wave-packet evolves into an IS state (see Fig. 3).

the IS, it is instructive to comment first an analogy with a nonlocal spatial response. This analogy becomes apparent by remarking that Eq.(1) is almost identical to the non-local NLS equation, provided one substitutes the temporal response with a spatial nonlocal response,  $R(t) \rightarrow U(x)$  [15–17]. The fundamental difference is that nonlocal effects are not constrained by the causality condition, so that  $U(x)$  is an even function. Assuming the beam intensity approximately symmetric ( $N(x)$  is even), then the self-consistent potential  $V(x) = -\sigma U * N$  is also even. It becomes apparent that in the focusing regime ( $\sigma = +1$ ), the optical beam can be self-trapped by its own induced potential ( $V(x) < 0$ ). Conversely, in the defocusing regime ( $\sigma = -1$ ) the repelling potential leads to the expected beam spreading (see Fig. 4a-b).

*Non-inertial reference frame* – As commented above through Fig. 3, the spectral-shift of the wave-packet, with spectral velocity  $\alpha$ , leads to a constant acceleration of the IS. It thus proves convenient to study the dynamics of the wave-packet in its own accelerating reference frame

$$\xi = z, \quad \tau = t - \alpha z^2, \quad \Omega = \omega - \alpha z. \quad (3)$$

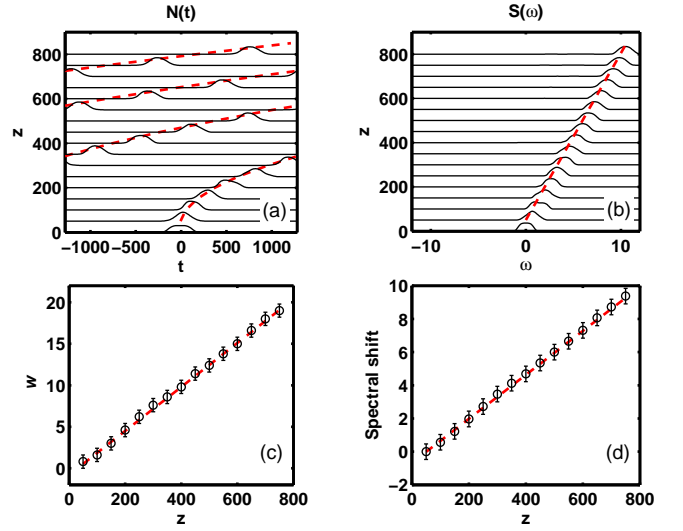


FIG. 3: Parabolic trajectory of the intensity profile  $N(t, z) = (2\pi)^{-1} \int n_\omega(t, z) d\omega$  (a), and evolution of the spectral profile  $S(\omega, z) = \int n_\omega(t, z) dt$  (b), corresponding to the simulation of the Vlasov Eq.(2) reported in Fig. 2 (right column). The linear increase of the IS velocity  $w$  (constant acceleration) (c), results from the linear spectral shift of the IS (d): the slope of the dashed red line in (c) is twice the corresponding slope in (d), as expected from the group-velocity dispersion law,  $\partial_\omega k(\omega) = 2\omega$ .

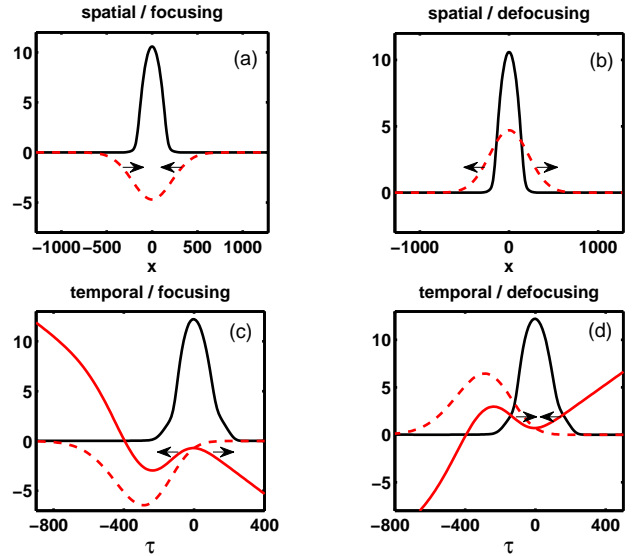


FIG. 4: Intensity profile  $N(x)$  (continuous dark line) and corresponding self-consistent potential  $V(x) = -\sigma U * N$  (dashed red line), in the case of a spatial nonlocal nonlinearity in the focusing (a), and defocusing (b), regimes. Intensity profile  $N(\tau)$  (continuous dark line), corresponding self-consistent potential  $V(\tau) = -\sigma R * N$  (dashed red line), and effective potential  $V_{\text{eff}}(\tau)$  [Eq.(5)] (continuous red line) in the accelerating reference frame, in the case of a temporal noninstantaneous nonlinearity in the focusing (c), and defocusing (d), regimes. The arrows indicate the ‘particle motions’ in the effective self-consistent potentials  $V_{\text{eff}}(\tau)$ : The non-inertial fictitious force inhibits (c) (induces (d)) the self-trapping in the defocusing (focusing) regime.

In this non-inertial reference frame the Vlasov Eq.(2) reads

$$\partial_{\xi} n_{\omega}(t, z) + 2\Omega \partial_{\tau} n_{\Omega}(\tau, \xi) - \partial_{\tau} V_{\text{eff}}(\tau, \xi) \partial_{\Omega} n_{\Omega}(\tau, \xi) = 0. \quad (4)$$

This equation remarkably *reveals the existence of an effective self-consistent potential*

$$V_{\text{eff}}(\tau, \xi) = V(\tau, \xi) + \alpha\tau, \quad (5)$$

where  $V(\tau, \xi) = -\sigma \int_{-\infty}^{+\infty} R(\tau - \tau') N(\tau', \xi) d\tau'$  just refers to the self-consistent potential written with the new variables (3). The linear part of the potential in (5) finds its origin in the fictitious force which results from the non-inertial nature of the reference frame, in analogy with the effective gravity mimicked by an elevator Ref.[28].

This fictitious force explains both phenomena of self-trapping with a defocusing nonlinearity, as well as the inhibition of self-trapping with a focusing nonlinearity. Let us first discuss the defocusing regime. Recalling that the potential is induced by the wave-packet itself, an IS can only form provided that *the self-induced potential  $V_{\text{eff}}(\tau)$  has a local minimum at the pulse center, i.e., at  $\tau = 0$  in the accelerating reference frame of the IS.* Contrary to the spatial case (Fig. 4a), it seems that this condition cannot be satisfied in the temporal case, since the causality condition shifts the potentials toward  $\tau < 0$ . However, in the defocusing regime, a local minimum can be restored at  $\tau = 0$  thanks to the fictitious force due to the non-inertial reference frame, as illustrated in Fig. 4d. More precisely, one can Taylor expand the effective potential  $V_{\text{eff}}(\tau) = a + (b + \alpha)\tau + c\tau^2 + \mathcal{O}(\tau^3)$  at  $\tau = 0$ , where  $b < 0$  in the defocusing regime and  $c > 0$  if the nonlinear response is slow enough (see Fig. 4d) [29]. In these conditions the particular choice  $\alpha_0 = -b$  guarantees that  $V_{\text{eff}}(\tau)$  has a local minimum at  $\tau = 0$  (see Fig. 4d). In other words, *the system spontaneously selects the amount of spectral shift,  $\alpha_0 = -\partial_{\tau} V|_{\tau=0}$ , and hence the amount of IS acceleration,  $2\alpha_0$ , in such a way that the effective self-consistent potential  $V_{\text{eff}}(\tau)$  admits a local minimum at  $\tau = 0$ .* This is confirmed by the numerical simulations of the Vlasov Eq.(4) reported in Fig. 4d, in which the value of  $\alpha_0 = 0.01325$

used to plot  $V_{\text{eff}}(\tau) = V(\tau) + \alpha_0\tau$  has been determined from the spectral shift measured in Fig. 3d. Note however that the potential barrier in the negative  $\tau$  axis is characterized by a limited depth, so that highly energetic particles can overcome such barrier to escape from the localized IS structure. Then depending on the initial condition and on the particular form of the response function, the phenomenon of incoherent self-trapping can be more or less efficient [29].

Let us now discuss the focusing regime, which is characterized by a red-shift of the wave-packet,  $\alpha < 0$ . Following the same reasoning as above and remarking that we now have  $b > 0$  and  $c < 0$ , the choice  $\alpha_0 = -b$  still leads to an extremum of  $V_{\text{eff}}(\tau)$  at  $\tau = 0$ . However, contrary to the defocusing regime, this extremum refers to a local maximum, as illustrated in Fig. 4c. Note that, in order to clearly differentiate the focusing and defocusing regimes, the IS profile  $N(\tau)$  of Fig. 4d has been used in Fig. 4c to calculate  $V(\tau)$  and  $V_{\text{eff}}(\tau)$  in the focusing case. Actually, in the focusing regime, there is no value of  $\alpha$  such that  $V_{\text{eff}}(\tau)$  has a local minimum at  $\tau = 0$ . The local maximum around  $\tau = 0$  then plays the role of a repelling potential, which explains the temporal broadening of the incoherent pulse: the ‘unstable particles’ located near by  $\tau = 0$  are either attracted toward the local minimum at  $\tau < 0$ , or either pushed toward  $\tau > 0$  by the non-inertial force (see Fig. 4c). Let us finally remark that, in this focusing regime, we didn’t identify the existence of dark IS states. Note that the homogeneous noise background inherent to such dark IS can be modulationally unstable in the focusing regime [27].

*Conclusion* – We reported a novel mechanism of self-trapping of incoherent nonlinear waves with a defocusing nonlinearity which is described in detail by a long-range Vlasov equation. Note that the extension of these ISs to the spatiotemporal domain is expected to give rise to accelerating incoherent light-bullets sustained by a focusing nonlinearity and normal dispersion. In contrast with the expected process of thermalization of an incoherent optical wave [9, 30], these IS states constitute genuine nonequilibrium and nonstationary stable states of the turbulent field.

- 
- [1] M. Mitchell, Z. Chen, M. Shih, and M. Segev, Phys. Rev. Lett. **77**, 490 (1996); M. Mitchell and M. Segev, Nature (London) **387**, 880 (1997).
- [2] See, e.g., D.N. Christodoulides *et al.*, Phys. Rev. Lett. **78**, 646 (1997); M. Mitchell *et al.*, Phys. Rev. Lett. **79**, 4990 (1997); O. Bang *et al.*, Phys. Rev. Lett. **83**, 5479 (1999); M. Peccianti, G. Assanto, Opt. Lett. **26**, 1791 (2001); T. Hansson *et al.*, Phys. Rev. Lett. **108**, 063901 (2012).
- [3] D.N. Christodoulides *et al.*, Phys. Rev. E **63**, 035601 (2001).
- [4] For a review, see Y.S. Kivshar and G.P. Agrawal, *Optical Solitons : From Fibers to Photonic Crystals* (Ac. Press, 2003).
- [5] See, e.g., M. Soljacic *et al.*, Phys. Rev. Lett. **84**, 467 (2000); D. Anderson *et al.*, Phys. Rev. E **69**, 025601 (2004); A. Sauter *et al.*, Opt. Lett. **30**, 2143 (2005).
- [6] A. Hasegawa, Phys. Fluids **18**, 77 (1975); Phys. Fluids **20**, 2155 (1977).
- [7] D. Dylov, J. Fleischer, Phys. Rev. Lett. **100**, 103903 (2008).
- [8] J. Garnier *et al.*, J. Opt. Soc. Am. B **20**, 1409 (2003).
- [9] A. Picozzi, Opt. Exp. **15**, 9063 (2007).
- [10] J. Garnier, A. Picozzi, Phys. Rev. A **81**, 033831 (2010).
- [11] B. Hall *et al.*, Phys. Rev. E **65**, 035602 (2002).
- [12] A. Picozzi, M. Haelterman, Phys. Rev. Lett. **86**, 2010 (2001); A. Picozzi *et al.*, Phys. Rev. Lett. **92**, 143906 (2004); A. Picozzi, P. Aschieri, Phys. Rev. E **72**, 046606 (2005); M. Wu *et al.*, Phys. Rev. Lett. **96**, 227202 (2006).
- [13] A. Picozzi *et al.*, Phys. Rev. Lett. **101**, 093901 (2008); C. Michel, B. Kibler, A. Picozzi, Phys. Rev. A **83**, 023806 (2011); B. Kibler *et al.*, Phys. Rev. E **84**, 066605 (2011).
- [14] O. Cohen *et al.*, Phys. Rev. E **73**, 015601 (2006); C. Rotschild *et al.*, Nature Photon. **2**, 371 (2008).
- [15] A. Picozzi, J. Garnier, Phys. Rev. Lett. **107**, 233901 (2011).
- [16] See, e.g., T. Lahaye *et al.*, Rep. Prog. Phys. **72**, 126401 (2009); S. Skupin, M. Saffman, W. Krolikowski, Phys. Rev. Lett. **98**, 263902 (2007); C. Conti, M. Peccianti, G. Assanto, Phys. Rev. Lett. **92**, 113902 (2004).
- [17] For a review, see W. Krolikowski *et al.*, J. Opt. B: Quant. Semicl. Opt. **6** S288 (2004).

- [18] A. Snyder, D. Mitchell, *Science* **276**, 1538 (1997).
- [19] V.E. Zakharov *et al.*, *JETP Lett.* **48**, 83 (1988); B. Rumpf, A.C. Newell, *Phys. Rev. Lett.* **87**, 054102 (2001); K. Hammani *et al.*, *Phys. Lett. A* **374**, 3585 (2010).
- [20] V. E. Zakharov, S. L. Musher, and A. M. Rubenchik, *Phys. Reports* **129**, 285-366 (1985).
- [21] M. Onorato *et al.*, *Phys. Rev. E* **67**, 046305 (2003).
- [22] C. Conti *et al.*, *Phys. Rev. Lett.* **105**, 263902 (2010).
- [23] In this regime, the response function,  $R(t)$ , cannot be expanded as in the usual treatment of the Raman effect in optical fibers [4].
- [24] For a discussion of the properties of a spectrogram, see J. Dudley *et al.*, *Rev. Mod. Phys.* **78**, 1135 (2006). The spectrograms in Figs. 1-2 refer to a sech-shaped window function whose FWHM  $\Delta_0 = \tau_c$ , where  $\tau_c$  is the time correlation. Whenever  $\Delta_0 \sim \tau_c$ , the particular choice of  $\Delta_0$  affects the resolution of the spectrogram without altering its global shape.
- [25] A spectral blue-shift induced by a delayed nonlinear response is well-known, e.g., in plasma: A. Couairon, A. Mysyrowicz, *Phys. Rep.* **441**, 47 (2007); M.F. Saleh *et al.*, *Phys. Rev. Lett.* **107**, 203902 (2011).
- [26] J. Garnier, M. Lisak, A. Picozzi, *J. Opt. Soc. Am. B* **29**, 2229-2242 (2012).
- [27] B. Kibler *et al.*, *Opt. Lett.* **37**, 2472 (2012).
- [28] A.V. Gorbach and D.V. Skryabin, *Nature Photon.* **1**, 653 (2007); *Phys. Rev. A* **76**, 053803 (2007).
- [29] Assuming  $N(t)$  approximately Gaussian with variance  $\Delta^2$  and  $R(t) \sim H(-t)t^s \exp[-t^2/(2\tau_R^2)]$ , the condition  $c > 0$  reads  $\tau_R > \Delta/\sqrt{s}$ .
- [30] See, e.g., B. Barviau *et al.*, *Opt. Express* **17**, 7392 (2009); *Phys. Rev. A* **79**, 063840 (2009); P. Suret *et al.*, *Phys. Rev. Lett.* **104**, 054101 (2010).